Motion Control of Linear Pulse Motor for Artificial Heart

H. Yamada, T. Mizuno, Y. Izumi,
H. Wakiwaka, Y. Kataoka
Faculty of Engineering, Shinshu University
500 Wakasato, Nagano 380-8553, Japan
yamadah@gipwc.shinshu-u.ac.jp

Y. Kikuchi
Sankyo Seiki Manufacturing Co., Ltd.
5329 Shimosuwa-Machi, Suwa-Gun 393-8511, Japan

M. Karita, M. Maeda
Shinko Electric Co., Ltd.
100 Takegahana, Ise 516-8550, Japan

Abstract - This paper deals with the difference of the static and kinetic thrust characteristics of a linear pulse motor (LPM) without and with feedback control for a total artificial heart (TAH). In general, the kinetic thrust of a LPM without feedback control decreases as increasing the mover velocity. The kinetic thrust characteristics of the LPM with feedback control are improved approximately 30 % as compared with the LPM without feedback control in the high velocity range.

1. Introduction

A linear motor-driven total artificial heart (TAH) is a pulsatile heart driven by a linear pulse motor. The linear TAH has advantages of simpler transmission mechanisms and fewer components than the ordinary rotary motor-driven TAH, because the linear motor is capable of directly driving the reciprocating pusher plates [1]-[4].

An experimental evaluation of the LPM without feedback control was carried out in an acute animal experiment in 1996. In that experiment, the TAH maintained an artificial circulation for only 2 h because of lack of kinetic thrust in the linear pulse motor (LPM) without feedback control. Therefore, a more powerful LPM than the LPM without feedback control is strongly required for TAH [5].

This paper describes the following aspects of the newly developed LPM with feedback control for TAH.

(1) Basic structure of the TAH and the LPM.
(2) Constitution of the control system of the LPM.
(3) Control performance of the LPM.

2. Structure of LPM for Total Artificial Heart

The basic structure of the linear motor-driven total artificial heart (TAH) is shown in Fig. 1 [6]. The TAH has two blood pumps, which are inflated and deflated by the LPM drive alternately, causing pusher plates to pulsate the blood. The two sac type blood pumps have four Jelly-fish valves [7].

Fig. 2 shows the basic structure of the LPM for a total artificial heart. The LPM consists of upper and lower pairs of stators (primary members) with a mover according to the reciprocating motion of the pusher plates attached to the mover (secondary member). The pitch of tooth τ = 0.8 mm. The support mechanism is very endurable, and linear bearings with eternally circulating balls support

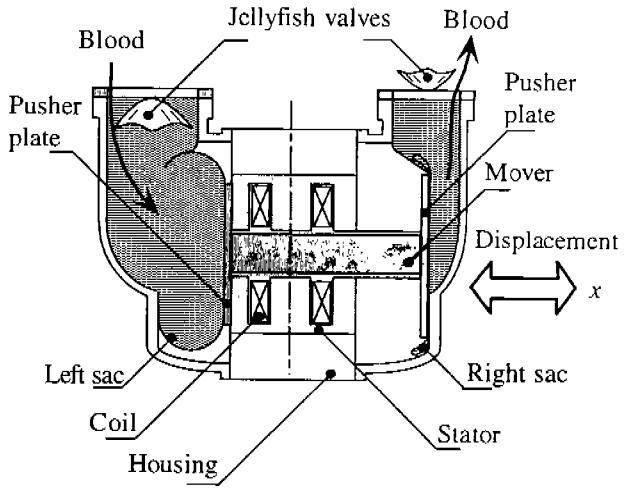

Fig. 1 Basic structure of the linear motor-driven total artificial heart.

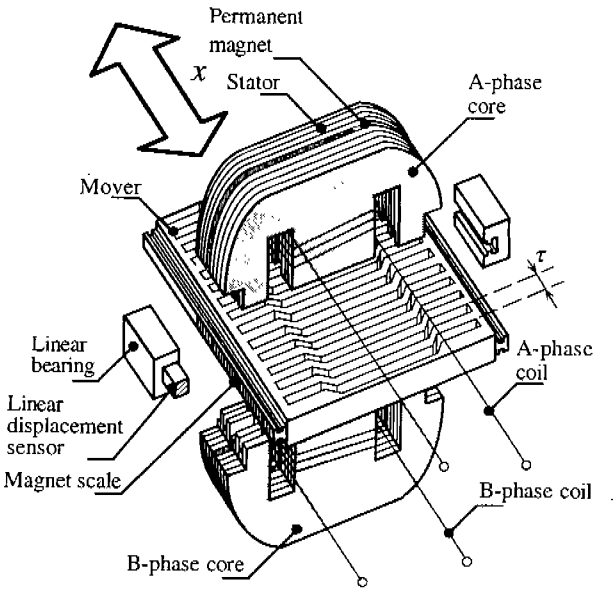

Fig. 2 Structure of the LPM with feedback control for total artificial heart (x is displacement).

gap of 40 μm between the primary and secondary sides. A linear displacement sensor using four magneto-resistive (MR) elements are attached to the linear bearing. Mechanical specifications of the LPM are listed in Table 1. The stators are laminated with Permendur

Table 1 Mechanical specifications of the linear pulse motor for total artificial heart.

	Item	Value	(Unit)
Stator (primary)	Number of teeth	16	per phase
	Pitch	0.8	(mm)
	Width of teeth	0.32	(mm)
	Width of slot	0.48	(mm)
	Length of tooth	56	(mm)
Mover (secondary)	Pitch	0.8	(mm)
	Width of tooth	0.32	(mm)
	Width of slot	0.48	(mm)
	Length of tooth	56	(mm)
Stroke		23	(mm)
Length of air gap		40	(μm)
Volume		206	(mL)
Mass		1400	(g)
Primary member		: 49%Co-2%V-Fe	
Secondary member (base)		: Carbon steel block	
(slit)		: 49%Co-2%V-Fe	

Table 2 Electromagnetic specifications of the linear pulse motor for total artificial heart.

Item	Value	
Number of pole	16	per phase
Number of turns (coil)	110	turns/phase
Exciting current	1.4	(A)
Magnetomotive force	200	(A/phase)
Resistance of coil	0.89	(Ω/phase)
Plastics magnet	Sm-Co	

(49%Co-2%V-Fe), and the mover consists of the magnetic poles made of Permendur and carbon steel block. Permendur is material featuring high saturation magnetic flux density, permeability and anti-vibration characteristics.

Electromagnetic specifications are listed in Table 2. The permanent magnet is a plastic cobalt magnet of rare earth.

3. Control system for the LPM

3.1 Constitution of the Linear Displacement Sensor Using MR Element

The linear displacement sensor for the feedback control is composed of a magnet scale and four magneto-resistive (MR) elements as shown in Fig. 3 [8][9][10]. The magnet scale is buried in the linear bearing, and moves with the LPM mover. The MR elements are made of the ferromagnetic material. The sensor can be

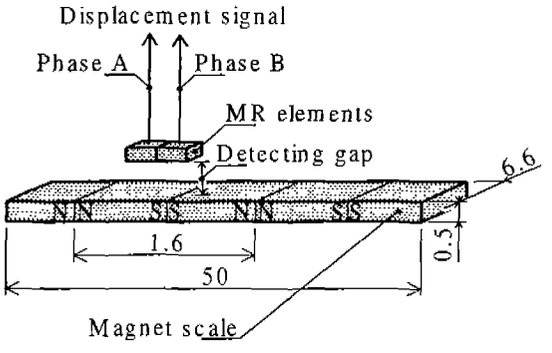

Fig. 3 Constitution of the linear displacement sensor using MR element for the linear pulse motor (unit is mm).

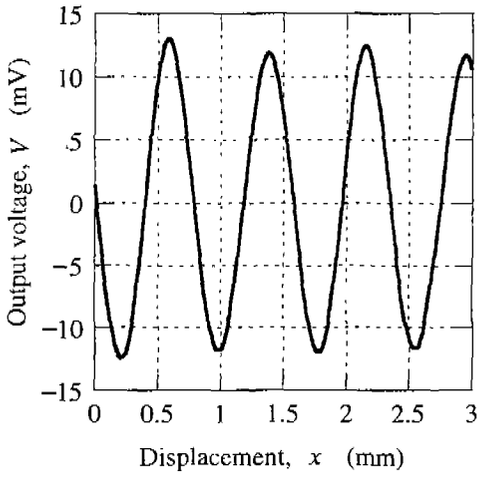

Fig. 4 Signal of linear displacement sensor using MR element for the linear pulse motor.

worked in the wide range of temperature. The bridge circuit is composed by the four magneto-resistive elements being used. Fig. 4 shows the signal of the linear displacement sensor. The waveform of the bridge output is shaped, and the displacement signal is fed back to the servo-driver.

3.2 Control System for the LPM

The expression of static thrust, F_s, of the LPM in the one-phase excitation is given by following equation [11]:

$$F_s = \frac{2\pi NI}{\tau} \Delta\Phi_m \sin\left(\frac{2\pi x}{\tau}\right) \quad \text{(N)}, \tag{1}$$

where NI is the electromagnetic force (A), τ is the pitch (m) of the LPM, $\Delta\Phi_m$ is the flux increment (Wb) by permanent magnet, and x is the displacement (m).

Fig. 5 shows the constitution of the feedback control system for the LPM. This system consists of the LPM and servo-driver, and the displacement signal of the LPM mover is feedback to the servo-driver. According to the system of the LPM for the linear pulse motor, mover displacement, exciting current I_a and I_b flow to the coil A and coil B respectively as follows:

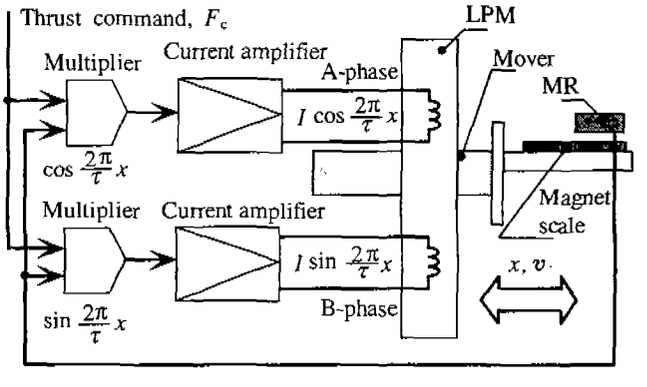

Fig. 5 Constitution of the feedback control system to the LPM.

$$I_a = I \sin\left(\frac{2\pi x}{\tau}\right) \quad \text{(A)}, \tag{2}$$

$$I_b = I \cos\left(\frac{2\pi x}{\tau}\right) \quad \text{(A)}, \tag{3}$$

where I is the exciting current (A).

Static thrust F_s of the LPM with feedback control is given by [11]:

$$F_s = K_f I_a \sin\left(\frac{2\pi x}{\tau}\right) + K_f I_b \cos\left(\frac{2\pi x}{\tau}\right), \\ = K_f I \quad \text{(N)}, \tag{4}$$

where K_f is the thrust constant (N/A).

4. Control Performance of the LPM

Fig. 6 shows the maximum static thrust, F_{sm}, versus the exciting current, I, characteristics of the LPM. The maximum static thrust of 102 N is obtained under the two-phase excitation at the rated current of 1.4 A. The value of thrust/input, F_s/P, is highest up to now. In general, the kinetic thrust of LPM without feedback control decreases following as the mover velocity increases. An approximate expression for the kinetic thrust, F_k, of the LPM without feedback control is described as [12]:

$$F_k = k F_{sm} \left\{1 - C\left(\frac{v}{v_m}\right)^2\right\} \quad \text{(N)}, \tag{5}$$

where k is the structure factor of the LPM, F_{sm} is the maximum static thrust (N), C is a factor due to the magnetic material, v is the velocity, and v_m is the maximum velocity (m/s).

The kinetic thrust characteristics of the LPM without feedback control is shown in Fig. 7. Maximum static thrust, F_{sm}, of the LPM is 102 N. Maximum kinetic thrust is 61 N in the velocity range from 10 mm/s to 200 mm/s.

Fig. 8 shows the kinetic thrust, versus the exiting current characteristics of the LPM without feedback control, when the velocity is 100 mm/s. The kinetic thrust F_k is not more than 60 % as compared with the maximum static thrust of the LPM because of the step-out of LPM without feedback control.

Fig. 9 shows the kinetic thrust characteristics of the LPM with feedback control. The kinetic thrust with feedback control increase at low velocity. However on high velocity, especially more than 170 mm/s, the kinetic thrust

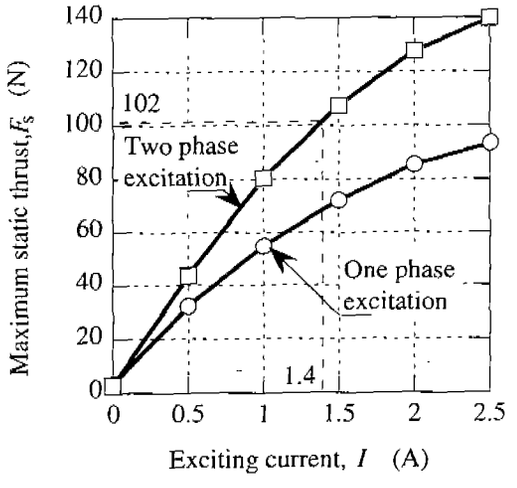

Fig. 6 Maximum static thrust, F_{sm}, versus the exiting current, I, characteristics of the LPM.

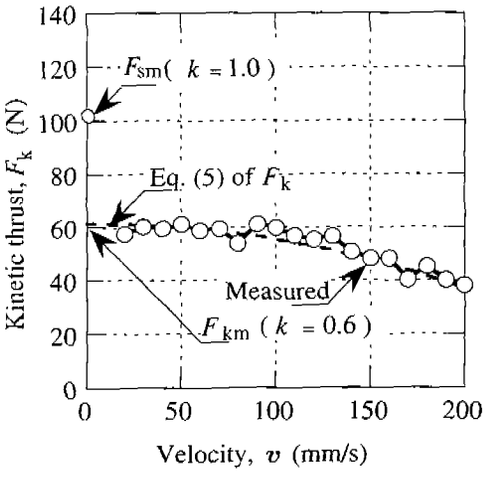

Fig. 7 Kinetic thrust characteristics of the LPM without feedback control ($k = 0.6$, $C = 0.4$).

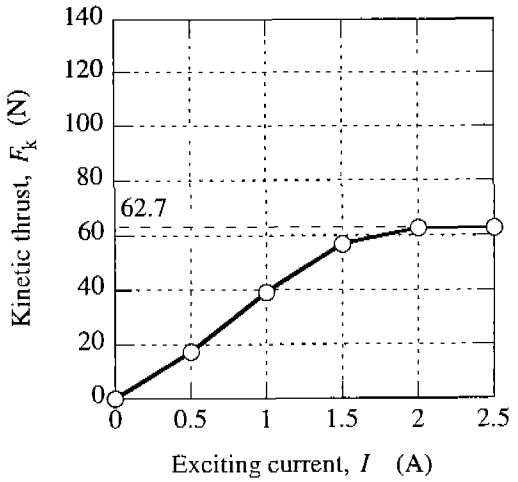

Fig. 8 Kinetic thrust, F_k, versus the exiting current, I, characteristics of the LPM without feedback control (v =100 mm/s).

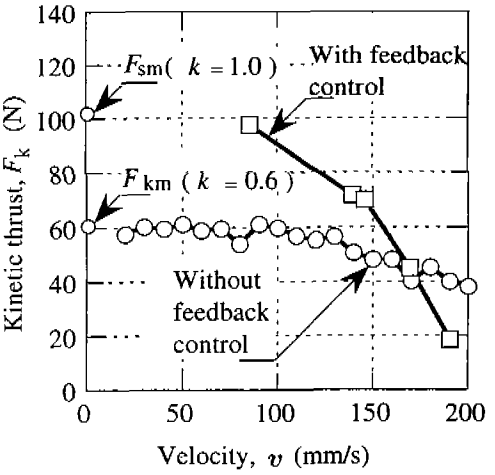

Fig. 10 Comparison of the kinetic thrust characteristics of the LPM with and without feedback control (I = 1.4 A constant, respectively).

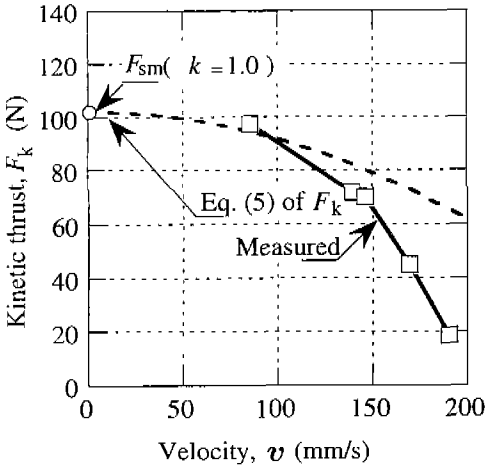

Fig. 9 Kinetic thrust characteristics of the LPM with feedback control (k = 1.0 , C = 0.4).

of the LPM with feedback control is least than that of the LPM without feedback control.

Fig. 10 shows the comparison of the kinetic thrust characteristics of the LPM with and without feedback control. Because of the displacement sensor's vibration, kinetic thrust of the LPM with feedback control decrease with increasing velocity.

5. Conclusion

Comparison of the kinetic thrust characteristics of a linear pulse motor without and with feedback control was discussed based on experimental data.

The output voltage of newly developed small-sized linear displacement sensor (3.7×12 × 2.95 mm) using MR element was synchronized with the position of the mover. When the velocity, v, of the mover was 100 mm/s, i.e. pulse rate of 75 beats /mm, the kinetic thrust of the LPM with feedback control was 90 N larger than without control of 60 N.

The key point of the kinetic thrust characteristics will be suppression of gap vibration between the sensor and the LPM.

References

[1] M. Karita, H. Nakagawa, M. Maeda, H. Yamada, and K. Kawakatsu: Development of double sided linear pulse motor, IEEE Transactions on Magnetics, Vol. 25, pp. 3257

3259, 1989.
[2] H. Yamada, M. Kobayashi, M. Watanabe, M. Yamaguchi, M. Karita, M. Maeda, S. Fukunaga: Performance characteristics of a linear motor-driven total artificial heart for second step, 1st International Symposium on Linear Drives for Industry Applications, LDIA'95, pp. 453-456, 1995.
[3] H. Yamada, M. Yamaguchi, K. Kobayashi, Y. Matsuura, and H. Takano: Development and test of a linear motor-driven total artificial heart, IEEE Engineering in Medicine and Biology, Jan./Feb, pp. 84 - 90, 1995.
[4] H. Yamada, M. Kobayashi, M. Watanabe, H. Wakiwaka, M. Karita, M. Maeda, Y. Matsuura, S. Fukunaga, and H. Hotei: Second type of linear motor-driven total artificial heart, Heart Replacement-Artificial heart 5 (Ed. by T. Akutsu and H. Koyanagi) Springer-Verlag Tokyo, pp. 121-124, 1996.
[5] M. Kobayashi, H. Yamada, T. Mizuno, H. Mizuno, M. Karita, M. Maeda, Y. Matsuura, and S. Fukunaga: Use of an improved linear motor-driven total artificial heart in an acute animal experiment, Heart Replacement-Artificial heart 6 (Ed by T. Akutsu and H. Koyanagi) Springer-Verlag Tokyo, pp. 21-25, 1998.
[6] H. Yamada: Study on linear motor application to total artificial heart drive, Hiroshima University Journal of Medicine, Vol. 46, No. 1, pp. 25-37, 1998 (in Japanese).
[7] K. Imachi, K. Mabuchi, T. Chinzei, Y. Abe, K. Imanishi, T. Yonezawa, K. Maeda, M. Suzukawa, A. Kouno, I. Fujimasa, and K. tsumi: Invitro and in vivo evaluation of a jellyfish valve for practical use, ASAIO Trans., Vol. 35, pp. 298-301, 1989.
[8] Y. Kikuchi, F. Nakamura, H. Wakiwaka, H. Yamada and Y. Yamamoto: Consideration of magnetization and detection on magnetic rotary encoder using finite element method, IEEE Trans., Magnetics., Vol. 33, No. 2, pp. 2159-2162, 1997.
[9] Y. Kikuchi, K. Shiotani, F. Nakamura, H. Wakiwaka, and H. Yamada: Examination to make highly accurate encoder using a magneto-resistive element, Proceedings of Sensors, Transducers and Systems (SENSOR'97), No. 1, pp. 31-36, 1997.
[10] Y. Kikuchi, Y. Kataoka, K. Shiotani, H. Wakiwaka, H. Yamada: Distortion factor of MR output with varied positions of magnetic encoder for LPM, 1998 National Convention Record IEE Japan —Industry Applications Society—, pp. 367-368, 1998 (in Japanese).
[11] T. Mizuno, H. Yamada, S. Yamamoto, M. Yamamoto, Y. Chang: Improved dynamic characteristics of linear pulse motor and application to the back gauge of the bending machine, IEEJ, Trans., Vol. 108-D, No. 10, pp. 903-910, 1988 (in Japanese).
[12] H. Yamada, M. Kobayashi, M. Watanabe, H. Mizuno, and M. Yamaguchi: Kinetic thrust analysis of a linear pulse motor, Journal of The Magnetics Society of Japan, Vol. 20, No. 2, pp. 617-620, 1996 (in Japanese).